

Detection of the Madden–Julian Oscillation in the Indian Ocean From Satellite Altimetry

Gary Grunseich and Bulusu Subrahmanyam

Abstract—The role of air-sea interaction on Madden–Julian oscillation (MJO) propagations across the tropical Indian Ocean is analyzed using integrated multimission satellite measurements of sea surface height and outgoing longwave radiation (OLR). MJO-related activity is observed in both parameters in the eastern equatorial Indian Ocean indicating a unique interaction in this region. In the eastern Indian Ocean, atmospheric conditions appear to aid in the creation of equatorial Rossby waves, while in the central and western Indian Ocean, different phases of oceanic Rossby wave propagations seem to have a strong influence on atmospheric conditions associated with the MJO. The downwelling phase of equatorial Rossby waves corresponds to a strengthening of OLR anomalies in extent and magnitude across the equatorial Indian Ocean, while the upwelling phase appears to weaken atmospheric MJO activity. This study improves climate research by identifying the MJO signal in altimetry data.

Index Terms—Altimetry, Indian Ocean, Madden–Julian oscillation (MJO), sea surface height (SSH).

I. INTRODUCTION

THE Madden–Julian oscillation (MJO) is a 30–80-day fluctuation in atmospheric and oceanic conditions that influences intraseasonal climate in the tropics [1], [2]. The possible connections and roles of air-sea interaction have been studied using sea surface variables such as temperature and salinity and many atmospheric variables ranging from satellite-derived winds, outgoing longwave radiation (OLR), and using global circulation models [3]–[6]. However, understanding the mechanisms responsible for initiating MJO propagations in the Indian Ocean is of growing interest along with the dynamics that result in fluctuations of MJO activity.

Sea surface height (SSH) measurements serve as an important resource to understand the sea surface conditions that may be responsible for triggering an MJO event. They are also an indicator of the possible impacts that atmospheric conditions associated with each phase of the MJO may have on oceanic features. Studies of the MJO using altimetric SSH have focused on the Kelvin wave response in the Pacific Ocean as shown in [7], but little attention has been given to the Indian Ocean region, which is an important site for MJO initiation. In [8], the effects of equatorial downwelling Rossby waves are shown

Manuscript received April 27, 2012; revised June 8, 2012; accepted July 5, 2012. Date of publication August 10, 2012; date of current version November 24, 2012. The work of G. Grunseich was supported in part by South Carolina Space Grant Consortium Graduate Fellowship. The work of B. Subrahmanyam was supported in part by the Office of Naval Research under Grant N00014-12-1-0454.

G. Grunseich is with the Department of Earth and Ocean Sciences, University of South Carolina, Columbia, SC 29208 USA (e-mail: ggrunseich@geol.sc.edu).

B. Subrahmanyam is with the Marine Science Program and the Department of Earth and Ocean Sciences, University of South Carolina, Columbia, SC 29208 USA (e-mail: sbulusu@geol.sc.edu).

Digital Object Identifier 10.1109/LGRS.2012.2208261

to create favorable conditions in the western Indian Ocean for the development of MJO-related convection. The deepening of the warm mixed layer provides an adequate resource for ocean surface heat flux into the atmosphere. However, as MJO-related convection propagates across the Indian Ocean, anomalous wind conditions produce reflecting downwelling Kelvin and Rossby waves along the Indonesian coast [9].

In this letter, the connection between long waves and MJO propagations is explored by examining the impact of both downwelling and upwelling Rossby waves on MJO activity across the Indian Ocean. The implications of atmospheric conditions on long-wave initiation are also analyzed. The main objective of this study is to use altimetry data to analyze the interaction of the MJO with surface ocean features.

II. DATA AND METHODS

The scope of this study is to understand the interaction of the MJO with the oceanic features that influence SSH. To resolve the different stages of MJO propagations across the Indian Ocean, OLR is used. To determine the different phases of large-scale oceanic waves, SSH data were filtered to resolve equatorial Kelvin and Rossby waves. Aviso SSH data, created by merging several satellite altimetry observations for the October 1992–December 2008 time period, were bandpass filtered to isolate the 30–100-day signal. We utilized the Reference series of Delayed-Time Maps of Sea Level Anomaly (Ref DT-MSLA) “Ref” series SSH data which have a 7-day temporal resolution on a 1/4° grid (<http://www.aviso.oceanobs.com/en/data/products/sea-surface-height-products/global/msla/index.html>). OLR data [10] for the overlapping period with SSH data from 15° S–15° N, 30° E–120° E were bandpass filtered using the Lanczos weights from [4] to isolate and define the MJO signal. MJO events were identified based on the number of well-defined peaks in OLR that passed over 0°, 90° E. Positive peaks (anomalous clear sky conditions) in OLR were designated as the 0-day stage of the MJO propagation. The methodology from [5] and [11] was followed in constructing MJO composites of OLR and SSH. Morlet wavelet analysis of OLR and SSH data for the 1993–2008 time period was performed at 0°, 90° E due to this particular location experiencing strong MJO-related activity during boreal summer and winter and in order to understand the interaction of the MJO and Kelvin waves. This type of analysis was also carried out in the western equatorial Indian Ocean in order to study the link between Rossby wave and MJO activity. We followed a similar wavelet analysis methodology shown in [12] and [13].

III. RESULTS

Wavelet analysis in the eastern equatorial Indian Ocean reveals a strong connection between MJO activity in OLR and

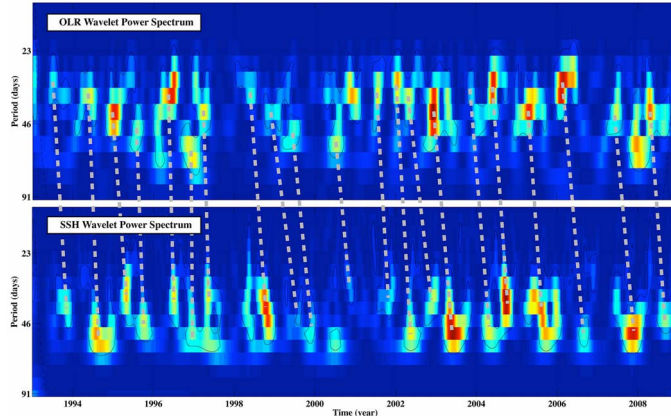


Fig. 1. Wavelet analysis of OLR and SSH averaged for 0° , 90° E. The wavelet power spectrum (the importance of a wave period at a given time). Corresponding pulses in peak MJO-related activity in OLR and SSH are shown using gray dashed lines.

SSH (Fig. 1). The top of Fig. 1 shows a total of 21 strong peaks in MJO-related activity in OLR during the 1993–2008 time period. Many of these peaks correspond to peaks in activity for SSH in this location (Fig. 1, bottom). Activity in this particular range of periods indicates that the MJO is forcing a Kelvin wave response in the eastern equatorial Indian Ocean. Time series of the maximum wavelet strength for both OLR and SSH were created, and peaks of the maximum activity were identified in both data sets. The time between SSH and OLR peaks in spectral activity shows that, when SSH lags peaks in OLR, there is, on average, a lag time of 51 days between the peaks compared to 86 days when OLR lags SSH peaks. The standard deviation of the time difference in peaks is lower when SSH lags OLR indicating that this lag is much more consistent compared to the higher standard deviations observed when SSH leads OLR peaks. The corresponding peaks in SSH and OLR activities are linked in Fig. 1 using this methodology. The average lag of 51 days corresponds to roughly one complete MJO propagation indicating that one MJO propagation may be necessary to create the oceanic conditions that invoke a Kelvin wave response in SSH.

Performing wavelet analysis in the western equatorial Indian Ocean demonstrates the interaction of Rossby waves and MJO-related activity in OLR. In Fig. 2, peaks in MJO-related activity in OLR (top) and Rossby wave activity in SSH (bottom) indicate that, during and shortly after 12 strong periods of Rossby wave activity, a strong atmospheric MJO response is induced. This could be due to different phases of Rossby wave propagations in this region reinforcing the conditions necessary to trigger enhanced convection or suppressed cloud cover during MJO propagations.

Analysis of OLR and SSH Hovmöller diagrams also reveals the interaction of oceanic and atmospheric properties. Fig. 3 shows a Hovmöller diagram of filtered OLR and SSH data during a 6-month period of 2001. This diagram reinforces the dynamics shown in [8] where a downwelling Rossby wave arrives in the western equatorial Indian Ocean creating favorable conditions for convective activity to develop. In Fig. 3, a downwelling Rossby (shown in orange-red) wave peaks between 50° E and 60° E in the equatorial Indian Ocean starting in early July 2001. This creates a warm deep mixed layer, which provides a strong heat flux aiding in the development of convection. Shortly after the downwelling Rossby wave's arrival, con-

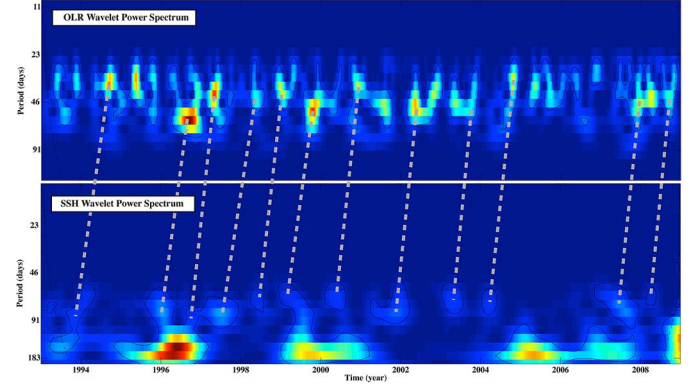


Fig. 2. Wavelet analysis of OLR and SSH averaged for 2.5° N– 5° N, 65° E– 70° E. The wavelet power spectrum (the importance of a wave period at a given time). Corresponding pulses in peak MJO-related activity in OLR and Rossby wave activity in SSH are shown using gray dashed lines.

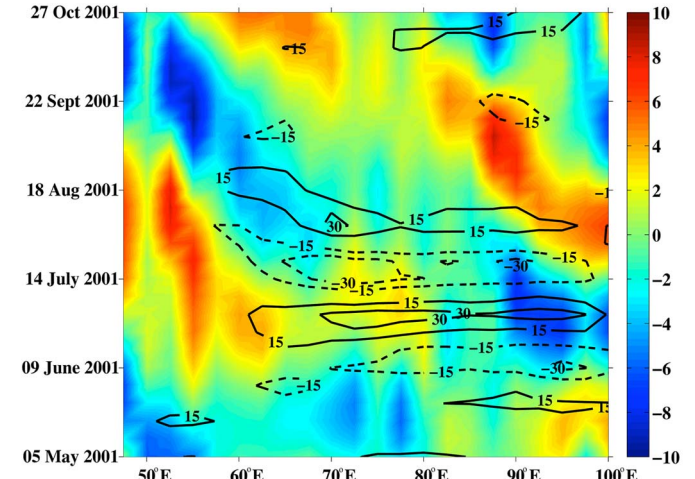


Fig. 3. Hovmöller diagram for the second half of 2001 showing filtered SSH anomalies (shaded in centimeters) and filtered OLR anomalies (contoured in watts per square meter) averaged from 2.5° N to 5° N. Upwelling equatorial Rossby waves are shown as negative SSH anomalies, while downwelling Rossby waves are shown as positive SSH anomalies.

vective activity (shown as dashed contours) is seen propagating eastward from the western equatorial Indian Ocean.

The 1994–1996 time period also demonstrates the air-sea interaction during MJO propagations. This particular period of time was chosen due to the consistency of Rossby waves traveling the length of the equatorial Indian Ocean rather than diminishing before reaching the western Indian Ocean and strength of the equatorial Rossby waves when compared to the rest of the time period. The connection between oceanic features and atmospheric conditions during MJO propagations can be observed by focusing on the different phases of Rossby wave propagations. When downwelling Rossby waves reach the central equatorial Indian Ocean (60° E– 80° E), there appears to be a strengthening in the magnitude of the OLR anomalies (Fig. 4). The strong OLR anomalies also appear to propagate the majority of the length of the equatorial Indian Ocean. During times of upwelling Rossby waves (shown in blue), weaker OLR anomalies appear across the Indian Ocean. The MJO propagations also appear to form in the western Indian Ocean and weaken before reaching the Indonesian coast, or they only appear in the eastern Indian Ocean. The deep warm mixed layer during

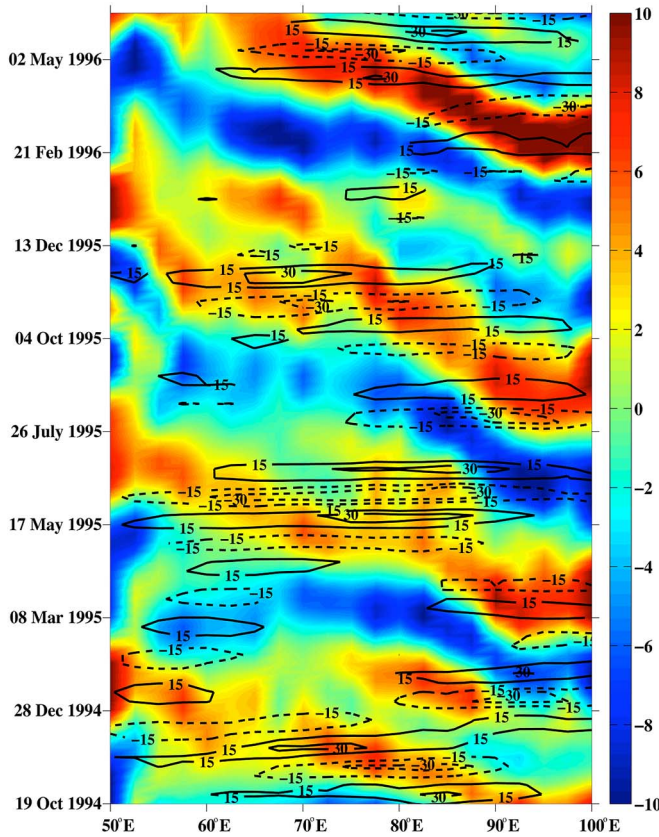


Fig. 4. Hovmöller diagram for the 1994–1996 time period showing filtered SSH anomalies (shaded in centimeters) and filtered OLR anomalies (contoured in watts per square meter) averaged from 2.5° N to 5° N. Upwelling equatorial Rossby waves are shown as negative SSH anomalies, while downwelling Rossby waves are shown as positive SSH anomalies.

downwelling Rossby waves creates favorable conditions for MJO propagations to extend the length of the Indian Ocean as well as strengthen while traveling east. Upwelling Rossby waves indicate a shallower cooler mixed layer, which may not support the propagation of strong MJO activity across the Indian Ocean.

Different phases of the MJO propagation across the Indian Ocean are analyzed using composite analysis of OLR and SSH data. Peaks in positive OLR anomalies at 0° , 90° E were used to define day 0. Data 10 and 20 days before and after the peak in OLR were then isolated to exhibit an entire MJO propagation across the Indian Ocean during the boreal winter months when the atmospheric component of the MJO is strongest. Using the MJO event dates from OLR, corresponding SSH data were composited for the entire time period. Fig. 5 (right) shows the OLR anomalies during different stages of the MJO propagation across the Indian Ocean. During lag -20 days, an upwelling Rossby wave forms off the coast of Indonesia (Fig. 5, left) and propagates westward across the equatorial Indian Ocean reaching the African coast by lag 10 days. Also, during the -20 -day lag, a downwelling Rossby wave can be observed in the central tropical Indian Ocean lasting through the day 0 lag. During lag 0 days, positive OLR anomalies peak in the eastern Indian Ocean corresponding with the formation of a downwelling equatorial Rossby wave in this region. This downwelling Rossby wave strengthens and propagates to the central Indian Ocean by lag 20 days. Fig. 5 reinforces the

dynamics observed in Figs. 3 and 4. Lag -20 days shows the remnants of an upwelling Rossby wave in the western equatorial Indian Ocean. Shortly thereafter (-10 days), positive OLR anomalies develop and propagate across the Indian Ocean and peak in the eastern Indian Ocean (0-day lag), which corresponds with the creation of a downwelling Rossby wave. The remnants of an earlier downwelling Rossby wave peak off the African coast during the 0-day lag, and within the next 10 days, negative OLR anomalies (the convective phase of the MJO) are created. The oceanic conditions associated with each phase of the equatorial Rossby wave during its propagation play a role in the enhancement of atmospheric conditions associated with a phase of the MJO. The atmospheric conditions in the eastern Indian Ocean may also be instrumental in aiding in the formation of a particular Rossby wave phase.

IV. DISCUSSION

Detection and analysis of the MJO signal in SSH are possible due to the limited variance of this measurement on seasonal and synoptic scales in the equatorial Indian Ocean allowing for intraseasonal features to be easily resolved. Analyzing SSH also demonstrates how the MJO forces equatorial Kelvin waves as well as the interaction of the MJO with the oceanic conditions associated with different phases of equatorial Rossby waves. Attention has recently been given to the interaction of Rossby waves and the atmospheric component of the MJO in [8]. Our study reveals that the MJO is influenced by Rossby waves on long time scales and across the equatorial Indian Ocean rather than just focusing on MJO initiation in the western Indian Ocean as shown in [8]. While the interaction between the MJO and Kelvin waves has been analyzed in previous studies, it is important to discuss the two types of large-scale oceanic waves in order to understand the dynamics between the ocean and atmosphere during MJO propagations.

Filtered SSH anomalies correspond to distinct oceanic properties. Downwelling equatorial Rossby waves create a deep warm mixed layer creating favorable conditions for convective activity. The magnitude and extent of MJO-related OLR anomalies appear to strengthen and increase in extent across the Indian Ocean during times of downwelling Rossby waves. Convection appears to weaken, and atmospheric conditions associated with MJO propagations appear to be disrupted during the westward propagation of upwelling equatorial Rossby waves. The shallower than normal mixed layer creates less favorable conditions for convection; thus, strong OLR anomalies do not appear to propagate across the entire tropical Indian Ocean under these conditions.

Wavelet analysis provides greater insight into the interaction between the atmospheric component of the MJO and equatorial Kelvin waves. During times of enhanced MJO-related activity in OLR in the eastern equatorial Indian Ocean, a lagged SSH response is observed in the Kelvin wave region of the spectrum. Analysis in the western equatorial Indian Ocean also demonstrates the interaction of Rossby waves and the atmospheric component of the MJO. This region demonstrates how Rossby wave activity in SSH leads MJO-related OLR activity.

Measurements gathered from the Dynamics of the MJO (DYNAMO) field campaign (from late 2011 to early 2012) will provide greater insight into interaction of the Indian Ocean

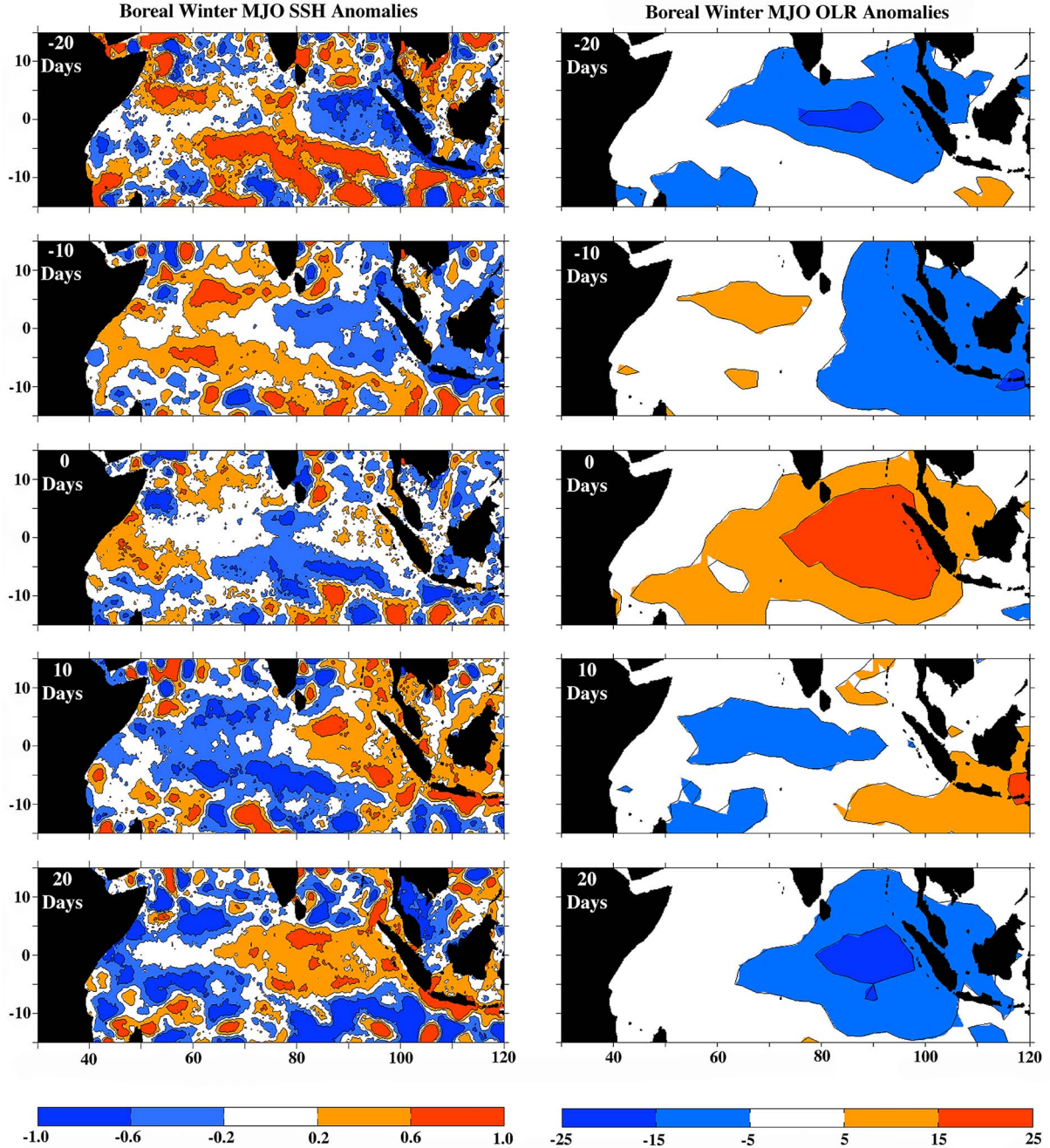


Fig. 5. Composite boreal winter MJO (left) SSH (in centimeters) and (right) OLR anomalies (in watts per square meter). SSH anomalies are taken with respect to the boreal winter mean.

and overlying atmosphere. Observational data will compliment satellite measurements that measure convection and SSH.

ACKNOWLEDGMENT

The authors would like to thank Aviso for making sea surface height data freely available. Interpolated outgoing longwave radiation data are provided by the National Oceanic and Atmospheric Administration's/Office of Oceanic and Atmospheric Research/Earth System Research Laboratory Physical Sciences Division, Boulder, CO, USA, from their Web site at <http://www.esrl.noaa.gov/psd/>. The authors would also like to thank the

Editor and three anonymous reviewers for their constructive comments that greatly improved this letter.

REFERENCES

- [1] R. A. Madden and P. R. Julian, "Detection of a 40–50 day oscillation in the zonal wind in the topical Pacific," *J. Atmos. Sci.*, vol. 28, no. 5, pp. 702–708, Jul. 1971.
- [2] M. C. Wheeler and H. H. Hendon, "An all-season real-time multivariate MJO index: Development of an index for monitoring and prediction," *Mon. Weather Rev.*, vol. 132, no. 8, pp. 1917–1932, Aug. 2004.
- [3] A. J. Matthews, P. Singhuruk, and K. J. Heywood, "Ocean temperature and salinity components of the Madden-Julian oscillation observed by Argo floats," *Climate Dyn.*, vol. 35, no. 7, pp. 1149–1168, Dec. 2010.

- [4] A. Arguez, M. A. Bourassa, and J. J. O'Brien, "Detection of the MJO signal from QuickSCAT," *J. Atmos. Ocean. Technol.*, vol. 22, no. 12, pp. 1885–1894, Dec. 2005.
- [5] G. Grunseich, B. Subrahmanyam, and A. Arguez, "Influence of the Madden–Julian oscillation on sea surface salinity in the Indian Ocean," *Geophys. Res. Lett.*, vol. 38, pp. L17605-1–L17605-9, Sep. 2011.
- [6] W. Han, D. Yuan, W. T. Liu, and D. J. Halkides, "Intraseasonal variability of the Indian Ocean sea surface temperature during boreal winter: Madden–Julian oscillation versus submonthly forcing and processes," *J. Geophys. Res.*, vol. 112, pp. C04001-1–C04001-20, Apr. 2007.
- [7] L. A. Edwards, R. E. Houseago-Stokes, and P. Cipollini, "Altimeter observations of the MJO/ENSO connection through Kelvin waves," *Int. J. Remote Sens.*, vol. 27, no. 6, pp. 1193–1203, Mar. 2006.
- [8] B. G. M. Webber, A. J. Matthews, K. J. Heywood, and D. P. Stevens, "Ocean Rossby waves as a triggering mechanism for primary Madden–Julian events," *Q. J. R. Meteorol. Soc.*, vol. 138, no. 663, pp. 514–527, Jan. 2011.
- [9] J. Vialard, S. S. C. Shenoi, J. P. McCreary, D. Shankar, F. Durand, V. Fernando, and S. R. Shetye, "Intraseasonal response of the northern Indian Ocean coastal waveguide to the Madden–Julian oscillation," *Geophys. Res. Lett.*, vol. 36, pp. L14606-1–L14606-5, Jul. 2009.
- [10] B. Liebmann and C. A. Smith, "Description of a complete (interpolated) outgoing longwave radiation data set," *Bull. Amer. Meteorol. Soc.*, vol. 77, pp. 1275–1277, 1996.
- [11] D. E. Waliser, R. Murtugudde, P. Strutton, and J. L. Li, "Subseasonal organization of ocean chlorophyll: Prospects for prediction based on the Madden–Julian oscillation," *Geophys. Res. Lett.*, vol. 32, pp. L23602-1–L23602-4, Dec. 2005.
- [12] C. Torrence and P. J. Webster, "Interdecadal changes in the ENSO–monsoon system," *J. Climate*, vol. 12, no. 8, pp. 2679–2690, Aug. 1999.
- [13] A. Grinsted, J. C. Moore, and S. Jevrejeva, "Application of the cross wavelet transform and wavelet coherence to geophysical time series," *Nonlin. Process. Geophys.*, vol. 11, no. 5/6, pp. 561–566, Nov. 2004.